CONF-840311--16

DE85 000895

COMPARISON OF ELECTRON CYCLOTRON HEATING THEORY AND EXPERIMENT IN EBT*

EBT Experimental Group
EBT Theory Group

Presented by

D. B. Batchelor

Oak Ridge National Laboratory
Oak Ridge, Tennessee 37830

INTRODUCTION

The ELMO Bumpy Torus (EBT) device consists of 24 simple mirrors joined end-to-end so as to form a closed field line torus. The mirror ratio in each simple mirror sector is 1.9:1. The device is heated by fundamental and second harmonic electron cyclotron resonance interaction. When operated at a central midplane magnetic field of 5 kG and microwave power up to 60 kW at 18 GHz, the device is called EBT-I. When operated at a central midplane magnetic field of 7.2 kG with microwave power up to 200 kW at 28 GHz, the device is referred to as EBT-S.

For most of the time that EBT has been in operation the experimental emphasis has been on confinement experiments and stability studies. Although electron cyclotron heating (ECH) is fundamental to EBT operation, it is difficult to measure wave fields in the plasma, heating rates, or other phenomena that give information directly about the wave physics. Hence, the study of ECH on EBT began as a theoretical program whose first objective was to understand the gross features of microwave power flow and power deposition

*Research sponsored by the Office of Fusion Energy, U.S. Department of Energy, under Contract No. W-7405-eng-26 with the Union Carbide Corporation.

in each of the plasma components. This was accomplished by using ray tracing /1,2/ techniques and by developing a zero-dimensional (0-D) wave energy balance model that takes into account the many passes through the plasma and essentially random reflections which a typical ray makes before being absorbed /3/. Over the last several years experiments have been performed with simple microwave calorimeters that are in good agreement with the power flow calculations for a wide variety of operating conditions /2/. Now we report experimental results that directly test and calibrate some of the assumptions of the power flow and absorption modeling. That is, the single-pass wave power absorption by the hot electron rings has been measured, the microwave losses to the EBT cavity walls have been measured, and the essentially complete opacity of the fundamental resonance to extraordinary mode waves propagating from the high-field side has been verified. In section 1 of this paper we outline the general features of microwave propagation and absorption in EBT and describe the most recent experiments.

Recent experiments and theoretical results indicate that confinement physics and heating physics in EBT devices are inextricably coupled. The picture that had previously emerged can be summarized as follows. An annular plasma of relativistic electrons ($T_A \sim 500$ keV) forms in a region near where the mod B contour for second harmonic resonance is tangent to a magnetic field line (Fig. 1). This relativistic electron component is diagnosed by hard X-ray detectors, synchrotron radiation, and diamagnetic loops. When the stored energy in the annuli becomes sufficiently large, flute instabilities associated with bad mirror curvature and plasma pressure are stabilized. It has conventionally been assumed that the stabilization mechanism is the formation of a radial magnetic well due to hot electron beta although other processes have recently been proposed /4/. The plasma radially outside the annuli, referred to as the surface plasma, is unstable and very poorly confined. The plasma radially inside the annuli is called the core plasma and is believed to be stable in the usual machine operating mode, the T-mode. For a discussion of EBT operating modes see Ref. /5/. Measurements of core plasma density using microwave interferometry and of core density and temperature using soft X-ray techniques at the mirror midplane indicated core densities somewhat less than $10^{12}/cm^3$ and temperatures in the range 200 to 1200 eV in EBT-S, depending on microwave power and gas feed rate.

The temperature of the "core" component was observed to scale with decreasing collisionality in a way which strongly suggested classical or neoclassical confinement. In particular, for collisionless electrons the

simplist neoclassical theory of Kovrizhnykh /6/ for bumpy tori that predicts an energy confinement time τ_E that scales as $\tau_E \propto T_e^{3/2}/n_e F(R_T, R_B, R_E, \ell)$, where F is a function of R_T = toroidal major radius, R_B = magnetic field ∇B scale length, R_E = ambipolar electric field scale length, and ℓ = plasma radius. Assuming that a constant fraction f of the input microwave power P_μ is absorbed by the core plasma, the power balance can be expressed as

$$P_\mu = \frac{n_e T_e}{\tau_E f} \propto \frac{n_e^2}{T_e^{1/2}} \frac{F(R_T, R_B, R_E, \ell)}{f} .$$

In experiments for which the neutral gas flow was adjusted so as to maintain constant plasma scale lengths, the quantity $n^2/T_e^{1/2}$ was indeed found to scale linearly with P_μ over a considerable range (Fig. 2). Also, the experimental densities and electron temperatures were consistent with 1-D transport modeling using more realistic transport coefficients and experimentally observed ambipolar potentials /7/.

Recent experiments however have shown that the core plasma confinement is considerably more complicated than is indicated by the midplane soft X-ray measurements. Thomson scattering measurements indicate that the bulk of the core density (50% to 90%) is composed of a collisional isotropic core component with T_e = 70–120 eV. Also, other recent experiments (mirror throat soft X-ray, throat-launched microwave power, and power feed turnoff experiments) demonstrate that the T_e = 200–1200 eV component seen by the midplane soft X-ray diagnostic is in fact a collisionless anisotropic hot tail. In section 2 we describe some of these experiments and give a theoretical interpretation of that data.

1. MICROWAVE POWER FLOW AND WAVE ABSORPTION

The microwaves in EBT-I (18 GHz) are injected from waveguides located at the midplane of each mirror sector. The 28-GHz power for EBT-S operation is distributed to each sector through a toroidal manifold which is fed by the gyrotron and serves simultaneously as an overmoded waveguide distribution system and a vacuum pumping manifold. In neither case is any directive or polarizing antenna structure present.

Numerous theoretical studies undertaken to elucidate the role of propagation and absorption processes in EBT have led to a qualitative understanding of ECH in EBT-I/S:

(1) Because of strong gradients in B along field lines, any extraordinary mode energy propagating from the high-field side of the fundamental resonance is totally absorbed. This is true even for the low density surface plasma.

(2) However, the extraordinary mode right-hand cutoff prevents extraordinary mode energy launched near the mirror midplane from propagating directly to the fundamental cyclotron resonance.

(3) The ordinary mode can propagate throughout the plasma, including the high-field region.

(4) A rapid equilibration between ordinary and extraordinary modes occurs due to mode conversion at wall reflection.

(5) The density and temperature of the core and surface plasmas in EBT-I/S are sufficiently small that absorption of the ordinary mode is quite small at both fundamental and second harmonic resonances.

(6) The extraordinary mode is moderately absorbed and the ordinary mode is weakly absorbed by the hot electron annuli.

The picture that emerges is one of weakly damped rays making many transits across the device, with wall reflections and repeated ordinary-extraordinary mode conversions playing an important role in the ultimate energy deposition. In order to deal with the complicated, essentially random nature of the wave propagation after a few wall reflections, a simple 0-D power balance model was developed that treated the sources, sinks, and conversion properties in a globally averaged way. The plasma is divided into regions bounded by cavity walls, resonant surfaces, or the right-hand cutoff surface. It is assumed that each mode propagates freely inside each region. At a wall boundary surface the waves are totally reflected and partially converted to the other mode. At a boundary surface in the plasma, waves can be reflected, partially absorbed, and partially transmitted to the adjacent plasma region. The power flux for each mode in each region is assumed to be isotropic in angle and uniform in space. Details of the 0-D model are given in Refs. /2,3/. Using this model we are able to estimate the wave energy density in each mode and the fraction of the total input power P_μ which is absorbed by each component. Using a combination of ray tracing calculations and the 0-D model we estimate that of the total power launched into the device during T-mode operation in EBT-S about 40% is deposited in the lossy surface plasma. This is because the surface plasma covers more than half of the fundamental resonance surface, and extraordinary mode energy is strongly absorbed there

even for comparatively small plasma density and temperature. Approximately 33% of P_μ is deposited directly in the core plasma and about 28% goes to the hot electron annuli.

The calculations of absorption by the annulus are carried out using a relativistic form of Poynting's theorem /2,8/:

$$\frac{d}{ds}\,|\underset{\sim}{S}| = \frac{4\pi}{c}\,\underset{\sim}{E}^{*}\cdot\underset{\approx}{\sigma}^{H}\cdot\underset{\sim}{E}\ .$$

Here, s is the arc length along a ray, $\underset{\sim}{S} = \mathrm{Re}[\underset{\sim}{E}^{*}\times(\underset{\sim}{n}\times\underset{\sim}{E})]$ = Poynting's vector, $\underset{\sim}{n} = c\underset{\sim}{k}/\omega$ = real refractive index, and $\underset{\approx}{\sigma}^{H}$ = Hermitian part of the relativistic conductivity tensor. The real refractive index and the electric field polarization eigenvectors are determined from the ray tracing code, which uses the cold plasma dispersion relation. In calculating $\underset{\approx}{\sigma}^{H}$ an isotropic relativistic Maxwellian distribution function is assumed:

$$F(p) = \frac{1}{m^3c^3}\,\frac{\rho n_A}{4\pi K_2(\rho)}\,\exp\left[-\rho\left(1+\frac{p_\parallel^2+p_\perp^2}{m^2c^2}\right)^{1/2}\right],$$

where $\rho = m_e c^2/T_A$ and $K_2(\rho)$ is the modified Bessel function. An arbitrary number of cyclotron harmonics can be retained and all Bessel functions containing finite Larmor radius effects are included without expansion. Now measurements have been made of the single-pass microwave transmission through the hot electron annuli.

The experiment involves transmitting a swept frequency (18- to 26-GHz) wave through the hot electron ring, across the EBT midplane, using a pair of highly directive horns. Measurement of the difference in transmission amplitude with and without the presence of a hot electron population allows a determination of the ring absorption. The 18-GHz (EBT-I) system was used for plasma heating because it allows the flexibility to turn a cavity feed off, thereby reducing the ring density. Simultaneous hard X-ray and perpendicular stored energy measurements were made of the rings to determine the ring density and temperature for fed and unfed cavities.

Single-pass ring absorption was measured with the polarization of the microwaves perpendicular and parallel to the magnetic field corresponding to the extraordinary and ordinary modes of propagation. The measurements were made at a pressure just above the T-M transition where the rings have a large stored energy but remain stable. The ring temperature and density were also

measured with the hard X-ray diagnostic. Figure 3 shows the measured transmission as a function of frequency with and without a ring present. Note the lower level of transmission with a ring present, indicating absorption. The detailed structure apparent in the transmission signals is primarily due to reflections, of the cavity walls, of the horn radiation that is not coupled in a single pass.

To calculate the fractional power absorption the two signals were digitally subtracted and divided by the signal present without a ring. This fraction decreases with frequency from about 12% at 18 GHz to about 5% at 26 GHz. The ray tracing calculations follow this downward trend but tend to give somewhat higher absorption. The agreement is relatively good if one takes the ring parameters to be $n_A = 1.2 \times 10^{11}/cm^3$, $T_A = 200$ keV, but the theoretical result is about a factor of 2 higher than the experiment if one takes $n_A = 1.7 \times 10^{11}/cm^3$, $T_A = 120$ keV.

For the O-mode, no significant change in transmission was observed with and without a ring present. The ray tracing code predicts a ring absorption less than 1% for the O-mode consistent with the measurement. In addition, the single-pass absorption was measured above the T-C transition pressure with and without a heating microwave feed for both the O- and X-modes. For both modes no change in transmission was observed, indicating that changes in the core or surface plasma caused by the lack of a microwave feed were not responsible for the change in transmission observed at lower pressure. We feel therefore that the agreement between the measured absorption and the ray tracing calculations is quite good and that the ring power deposition predicted by the power balance model should be accurate to within a factor of 2.

Single-pass microwave absorption by the plasma in EBT is sufficiently weak that the microwaves undergo multiple reflections from the cavity walls before being absorbed. With each reflection some of the microwave energy is dissipated in the aluminum cavity walls. A set of measurements was made to determine this loss by measuring the power coupled out of a 3-in. port in one of the cavities into a waterload microwave calorimeter. An intercavity transport code was used to predict the power coupled to the calorimeter for various cavity microwave feed configurations and losses due to microwave absorbing diagnostic portholes as a function of the single bounce wall loss coefficient.

The data were obtained with the torus filled with nitrogen to atmospheric pressure. The total microwave power fed to the torus was held to $\sim$400 W. The input microwave frequency was swept $\pm$25 MHz about the central 18-GHz

frequency in order to scramble standing wave modes, thereby spatially averaging the power received by the calorimeter.

Various power feed and porthole loss configurations were used during the measurement. Power was fed to the torus at different cavities or sets of cavities to study the transport to the cavity with the calorimeter. A second set of measurements was made after nine 4-in.-diam port covers were removed to artifically increase the microwave losses. The transport code was used to model the experimental results. It was found that a wall loss coefficient of 0.7% per wall bounce matched the data quite well.

To determine the power lost to the wall in the presence of a plasma the 0-D microwave power balance model was modified to include a wall loss coefficient. For a wall loss coefficient of 0.7% the power balance model predicts a total (multibounce) wall loss of $\sim$5% the input microwave power. Thus, the wall losses can be considered an almost negligible microwave loss.

In order to improve the efficiency of core plasma heating, a program was initiated to launch extraordinary mode power directly from the high magnetic field side of the fundamental resonance. Calculations using the 0-D power balance model predicted that improvement would be marginal unless two constraints were satisfied: (1) that the power be beamed toward the plasma center and (2) that the microwaves be highly polarized in the extraordinary mode. To meet these requirements a high-power, linearly polarized, directive launcher was developed /9/. The extraordinary mode is elliptically polarized when propagating at an oblique angle to the magnetic field. In order to launch the waves perpendicular to B such that the extraordinary mode is linearly polarized, it was necessary to "snake" the launcher through the fundamental resonance zone and launch back toward the resonant layer (Fig. 4). In initial experiments, up to 24-kW net power from the high-field launcher was delivered to the plasma. Preliminary experiments with a microwave calorimeter located on the low-field side of the cavity into which the power was directed indicate that virtually none of the throat-launched power penetrates to the low magnetic field side when the launcher is indeed on the high-field side of the resonance. However, if the field strength is lowered such that the resonance moves to a higher field than the launcher, very high power levels are received by the calorimeter. We believe this indicates that the throat launcher does indeed excite predominantly extraordinary mode and that the extraordinary mode power is absorbed in a single pass through resonance.

2. RECENT RESULTS IN CORE HEATING AND CONFINEMENT

There have been a number of improvements in the Thomson scattering diagnostic, resulting in an improved signal-to-noise ratio, a vastly increased data base with computer acquisition, and radial scanning capability. The experiments establish the existence of a cold electron component with temperature about one-third that given by soft X-ray measurements. Figure 5 shows T_e as determined by both soft X ray and laser as a function of gas pressure. The laser is sensitive to electrons primarily with energy below about 200 eV, whereas the soft X ray is most sensitive to electrons in the range 500 eV to 2 keV. Therefore, both diagnostics are compatible with the concept of a two-temperature distribution. In fact, data in the higher energy laser channels are consistent with the presence of an energetic tail although it is difficult to establish the density and temperature of such a tail component.

Another recent enhancement is the installation of split coils in some of the mirrors, which allows diagnostic access to the plasma in the mirror throats. Interferometer measurements at the throat indicate the plasma density to be nearly equal to that at the midplane throughout the T-mode of operation. However, $(n_e)_{throat}/(n_e)_{mid}$ drops as the T-M transition is approached. Measurements with a soft X-ray detector located at the throat show that an energetic component is indeed present with $(T_h)_{throat} \cong (T_h)_{mid}$ but with much smaller density $(n_h)_{throat} \lesssim 0.1(n_h)_{mid}$. We regard this as strong evidence that the low temperature bulk component is isotropic whereas the energetic tail is highly anisotropic. In addition, one can infer that the electric field along $\underline{B}$ is small.

There is also clear evidence that the tail component is locally produced at the fundamental cyclotron resonance. The cavity containing the midplane soft X-ray detector is not fed with microwave power since bremstrahlung associated with the hot electron ring would mask the soft X-ray emission from the ∿600-eV component. However, there is a flux of extraordinary mode power on the fundamental resonance surfaces in this cavity from adjacent cavities that are powered. Now, if the microwave power is removed from these adjacent cavities, the extraordinary mode power flux on the fundamental resonances of the soft X-ray cavity drops essentially to zero according to the power balance model described in the last section. Indeed, it is observed that the soft X-ray signal drops effectively to zero under these conditions.

This behavior can be understood theoretically if one carefully takes into account the correlation between the spatial structure of the microwave

electric field $\underset{\sim}{E}_\mu(\underset{\sim}{x})$ and the velocity space structure of the plasma distribution function $f(\varepsilon,\mu)$, where $\varepsilon = mv^2/2$ = particle energy and $\mu = mv_\perp^2/2B$ = particle magnetic moment. For fixed position along a magnetic field line s, the condition for fundamental cyclotron resonance including the Doppler effect is

$$v_\parallel^{res}(s) = \frac{\omega - \Omega_e(s)}{k_\parallel(s)} \quad ,$$

where $v_\parallel^{res}(s)$ is the parallel velocity necessary for resonance at location s and $k_\parallel(s)$ is the real part of the parallel wave number at s. As an extraordinary mode wave approaches the fundamental resonance from the high magnetic field side, absorption begins and wave power starts to decrease where the velocity for Doppler-shifted resonance is a few times the thermal speed, $v_\parallel^{res}(s) = O(v_e)$ with $v_e = (2T_e/m_e)^{1/2}$.

For a Maxwellian plasma the profile of wave power $P_\mu(s)$ can be obtained by solving the dispersion relation. For $k_\perp = 0$ this dispersion relation takes the simple form

$$n_\parallel^2 = 1 - \frac{\omega_{pe}^2}{\omega^2}\frac{1}{n_\parallel}\frac{c}{v_e} Z\left(\frac{\omega - \Omega_e}{k_\parallel v_e}\right) ,$$

where $n_\parallel = ck_\parallel/\omega$ is the refractive index and $Z(\xi)$ is the plasma dispersion function. Figure 6(a) shows profiles of $k_r(\Omega_e/\omega)$ and $k_i(\Omega_e/\omega)$ for extraordinary waves propagating parallel to the field in a Maxwellian plasma or density $n_e = 10^{12}/cm^3$ and temperature $T_e = 300$ eV. Shown in Fig. 6(b) is the wave power profile $P_\mu(\Omega_e/\omega)$ for various temperatures determined from

$$P_\mu\left(\frac{\Omega_e}{\omega}\right) = P_\infty \exp\left\{-\int_{s(\Omega_e/\omega)}^{\infty} ds'\, 2k_i\left[\frac{\Omega_e}{\omega}(s')\right]\right\} ,$$

Where we have approximated the magnetic field profile near resonance as $\Omega_e(s)/\omega = 1 + s/L$ (L = 20 cm for application to the central region of EBT-I/S). Defining $\delta(s) \equiv \Omega_e(s)/\omega - 1$, we see for example in the $T_e = 300$-eV case that 50% of the power is absorbed by $\delta = 0.07$ (s = 1.4 cm) and that 90% of the power is absorbed by $\delta = 0.04$ (s = 0.8 cm). The importance of this

observation is that only particles with comparatively large $v_\parallel$ are heated, i.e., those with $\delta^{res} \gtrsim 0.04$, where $P_\mu(s)$ is large.

The condition for resonance at a given location s or fractional shift δ away from the non-Doppler-shifted resonance, $v_\parallel^{res}(\delta) = -c\delta/n_\parallel(\delta)$, can be related to the energy and pitch angle at the mirror midplane. Invoking μ conservation gives

$$v_\parallel^{res}(\delta) = \pm\sqrt{\frac{\varepsilon}{2m}}\left(1 - \frac{v_{\perp 0}^2}{v^2}\frac{B^{res}}{B_0}\right)^{1/2} = \pm\sqrt{\frac{\varepsilon}{2m}}\left[1 - (1-\zeta^2)r(1+\delta)\right]^{1/2},$$

where B_0 = is the field strength at the midplane, $\zeta^2 = v_{\parallel 0}^2/v^2$, $v_{\parallel 0} = v_\parallel$ at the midplane, and $r = \omega/\Omega_{e0}$. Equating the two expressions for $v_\parallel^{res}$ and solving for the resonant energy we obtain

$$\varepsilon^{res}(\delta) = \frac{mc^2}{2}\frac{\delta^2/n_\parallel^2(\delta)}{1 - r(1+\delta)(1-\zeta^2)}.$$

It is important to note that to be resonant at a given δ there is a minimum required energy $\varepsilon_{min}^{res}(\delta) = 256\ \text{keV} \times \delta^2/n_\parallel^2(\delta)$ and that the minimum energy is obtained for purely passing particles, $\zeta = v_{\parallel 0}/v = 1$. The resonant energy increases with increasing μ, becoming infinite for particles turning just at the point δ. This somewhat counterintuitive result simply indicates that it is not sufficient to reach the magnetic field δ for an electron to be heated there; rather, it must also have $v_\parallel(\delta) = v_\parallel^{res}(\delta)$. For example, assuming $n_\parallel = 1.7$ and $r = 1.4$, which would be appropriate for a 2:1 mirror ratio as in EBT-S, for passing particles $\zeta = 1$ at $\delta = 0.07$ [the location at which half the power has been absorbed in the $T_e = 300$-eV case in Fig. 6(b)], one obtains $\varepsilon_{min}^{res} = 430$ eV. Also, for a trapped particle $\zeta \leq 0.707$ to be resonant at this location, it must have energy $\varepsilon^{res} = 1.7$ keV. We can conclude that if the bulk electron distribution in EBT were a Maxwellian at 300 eV most of the power would be absorbed by passing particles with energy above about $1.5T_e$ and by trapped particles with energy above about $6T_e$.

We see that there is considerable velocity space structure in the microwave heating operator. This comes about not only through the explicit velocity dependence but also because of the velocity dependence of the spatial location of the Doppler-shifted resonance and the strong spatial variation in wave power density due to heavy damping. Of course particles with

$\zeta \lesssim (1 - 1/r)^{1/2}$ (i.e., particles which turn before reaching resonance) are not heated at all.

The primary effect of fundamental extraordinary mode heating is to increase the electron's perpendicular energy at the resonance location. Parallel heating comes about only through μ conservation as the particle moves to lower magnetic field. Therefore, ζ tends to decrease as the heating progresses, passing particles become trapped, and trapped particles turn ever closer to the midplane, until electric field profile effects effectively shut off the heating. For the particles that are resonant at large values of δ, where the wave electric field is large, the heating is quite rapid. We can estimate the average heating rate as

$$\frac{\Delta\varepsilon_\perp}{\Delta t} = \frac{1}{\tau} \frac{\pi e^2 E_-^2}{2m\Omega_e} \frac{L}{v_\parallel}_{s^{res}} ,$$

where $\varepsilon_\perp$ is the perpendicular electron energy, E_- is the amplitude of the right circular component of the field, L is the magnetic field scale, τ is the transit time between successive passes through resonance, and s^{res} is the location of the Doppler-shifted resonance. Using parameters appropriate for EBT-S with 100 kW of ECH power (giving the asymptotic value for $E_- \cong 20$ V/cm), one obtains $\Delta\varepsilon_\perp/\Delta t \cong 3 \times 10^7$ eV/s. On the other hand, particles in the bulk of the distribution, $\varepsilon \lesssim T_e$, can only be heated by collisions with those energetic particles that are directly heated by the microwaves.

It is clear that the heating process has the potential for forming a cold, isotropic collisional bulk as well as an anisotropic, energetic tail in consonance with the experimental observations. Whether a significant tail actually forms depends upon how well the directly heated population is confined and how tightly the directly heated particles are collisionally coupled to the bulk. Now the confinement of energetic particles in EBT (i.e., particles with $\varepsilon > e\phi/a$, where E_0 is the ambipolar potential $\sim$100 to 400 V and a is the plasma minor radius) is very pitch-angle dependent. Since EBT relies on poloidal particle drifts Ω_D to cancel the vertical drift v_y due to toroidicity, those particles with small values of Ω_D have large neoclassical step sizes and large shifts inward in major radius, which can result in direct (i.e., nondiffusive) particle and energy loss. In particular, those particles that are transitional between trapped and passing tend to be very

lossy. This situation is illustrated in Fig. 7. The effect of the rf is to push passing or energetic trapped particles into the lossy region of velocity space.

Quantitative evaluation of these processes requires detailed modeling of the spatial dependence of the microwave field profiles and the velocity space dependence of power absorption by particles, collisional relaxation, radial diffusion of heat and particles, direct loss of heat and particles on open drift surfaces, and particle sources. Although this is an inherently 4-D problem, involving radial and poloidal variations as well as velocity space variations, we have initiated a program of Fokker-Planck modeling based on the 2-D finite-element code of Matsuda. The direct losses are being modeled as velocity-dependent particle sinks, and we hope to be able to model neoclassical radial diffusion in a similar manner. The preliminary results of this code indeed show the formation of an anisotropic tail and a cold collisional bulk component. In addition, the direct particle losses result in significant energy losses and reduction in bulk heating efficiency.

In summary we can see that the microwave power P_μ effectively vanishes near $\Omega_e(s) \cong \omega$. The implication of this is that for fixed ε passing particles are preferentially heated and for fixed pitch angle high energy particles are preferentially heated. The effect of the heating is to increase $v_\perp$, pushing passing particles toward the trapped-passing boundary where confinement is poor.

REFERENCES

/1/ BATCHELOR, D. B., and GOLDFINGER, R. C., Nucl. Fusion, 20 (1980) 403.

/2/ BATCHELOR, D. B., GOLDFINGER, R. C., and RASMUSSEN, D. A., Oak Ridge National Laboratory Report ORNL/TM-8770 (1983).

/3/ BATCHELOR, D. B., Nucl. Fusion, 21 (1981) 1615.

/4/ SPONG, D. A., Bull. Am. Phys. Soc., 28 (1983) 1228.

/5/ COLCHIN, R. J., et al., Plasma Phys., 25 (1983) 597.

/6/ KOVRIZHNYKH, L. M., Zh. Eksp. Teor. Fiz. (Sov. Phys. JETP), 29 (1969) 475.

/7/ HASTINGS, D. E., and KAMIMURA, T., accepted by Nucl. Fusion.

/8/ BATCHELOR, D. B., GOLDFINGER, R. C., and WEITZNER, H., Oak Ridge National Laboratory Report ORNL/TM-9075 (1984).

/9/ WHITE, T. L., invited paper this symposium.

FIGURE CAPTIONS

Fig. 1. Equatorial cross section of two EBT-S cavities.

Fig. 2. $\bar{n}_e^2/T_e^{1/2}$ as determined from midplane soft X-ray vs microwave power.

Fig. 3. Microwave transmission through a cavity midplane with and without a ring present.

Fig. 4. High-field, polarized extraordinary mode launcher "snaked" through the fundamental resonance.

Fig. 5. Core electron temperature as determined by midplane soft X-ray and laser Thomson scattering vs torus field pressure.

Fig. 6. (a) k-real and k-imaginary vs Ω_e/ω for parallel propagating extraordinary mode waves in a 300-eV Maxwellian plasma. (b) Wave power density profiles $\alpha|E_-|^2$ for various plasma temperatures.

Fig. 7. Velocity space geometry for ECH-enhanced neoclassical transport and direct particle loss in EBT.

ORNL–DWG 83-2528 FED

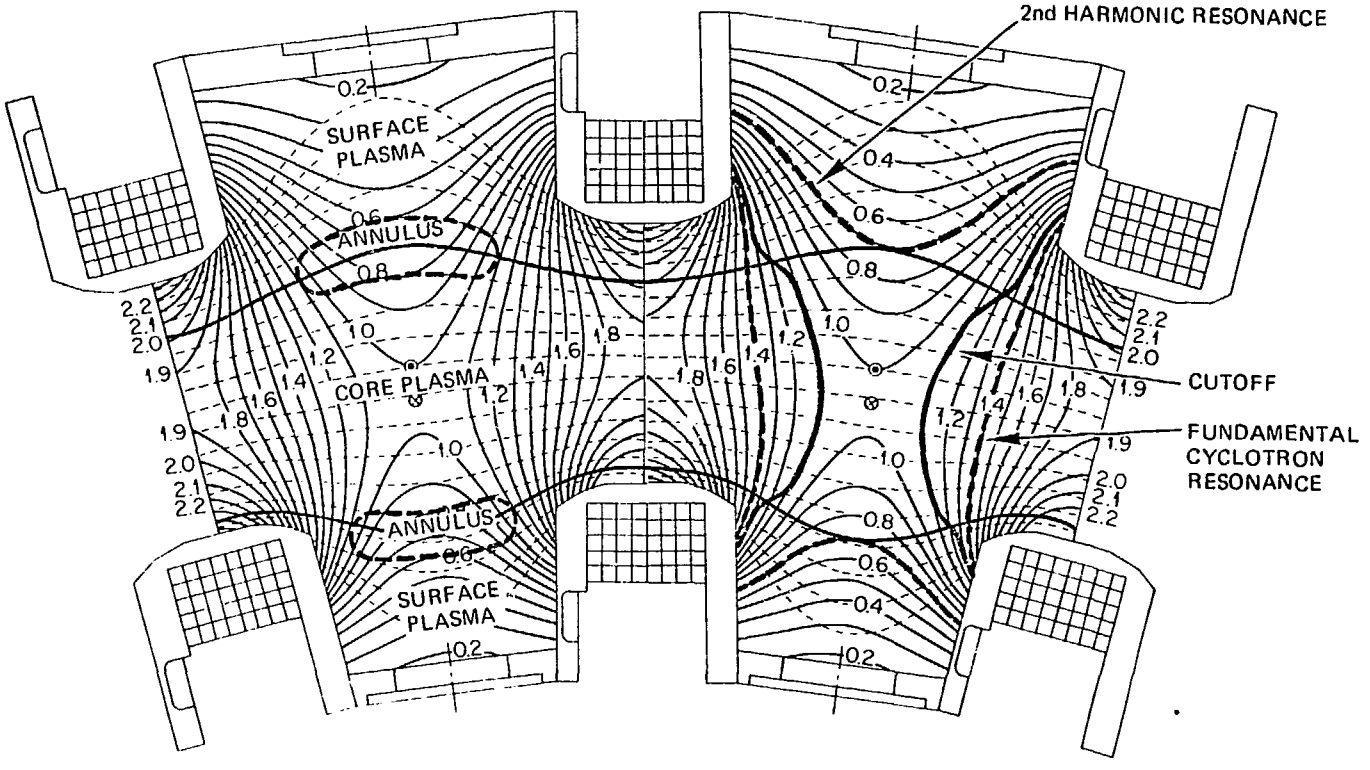

Fig. 1

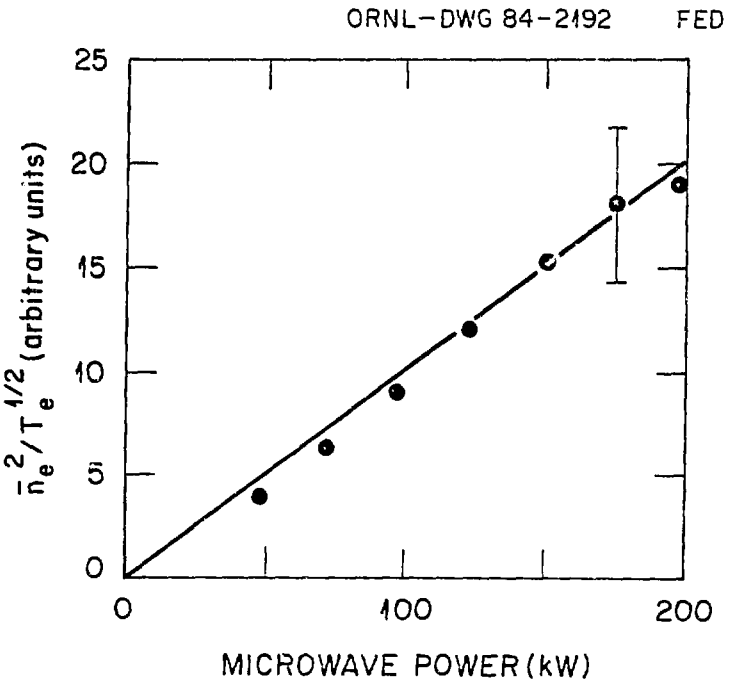
ORNL-DWG 84-2192 FED
25
20
15
10
5
0
0
100
200
MICROWAVE POWER (kW)
$\bar{n}_e^2 / T_e^{1/2}$ (arbitrary units)

Fig. 2

EXTRAORDINARY MODE
MICROWAVE TRANSMISSION vs FREQUENCY

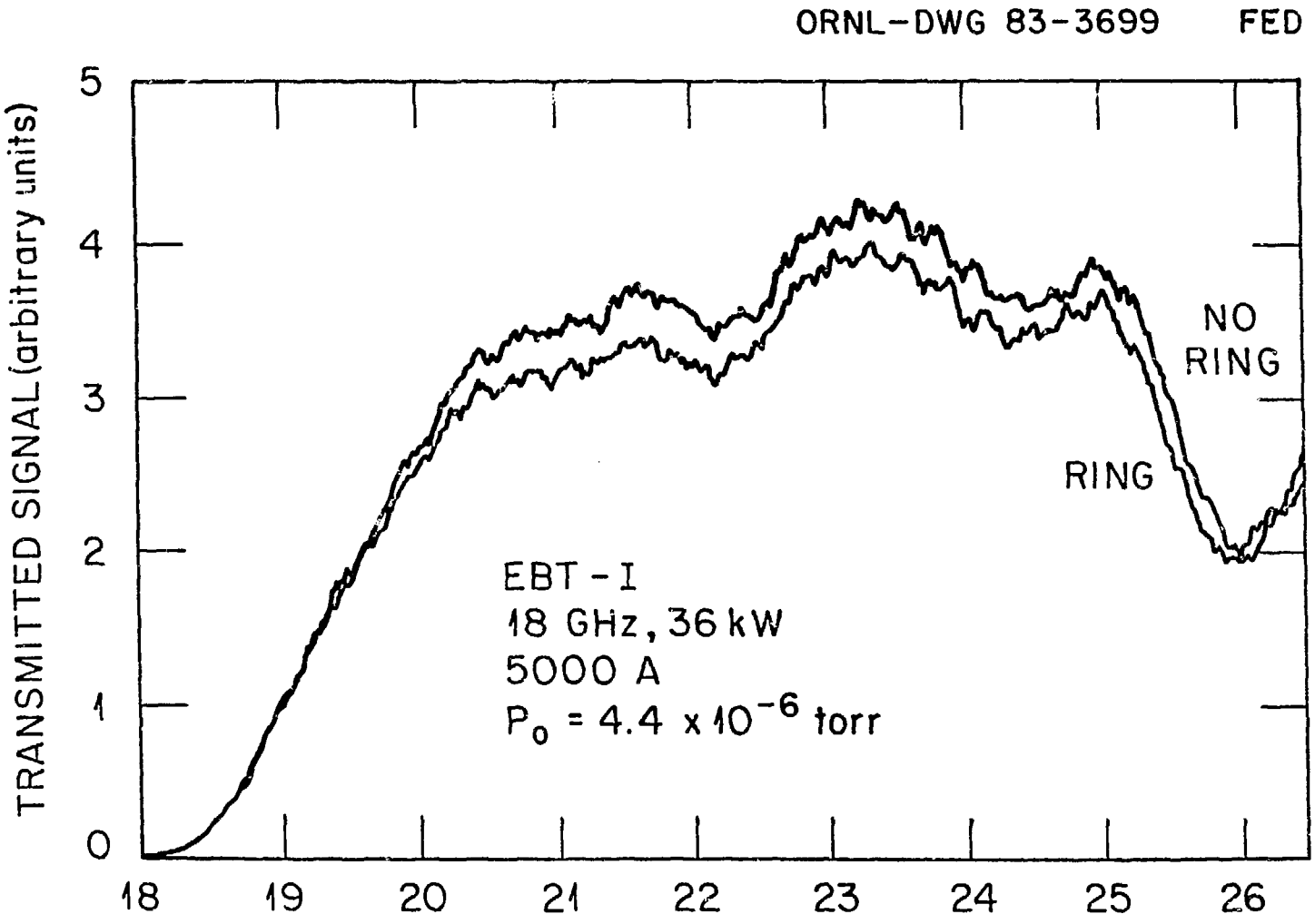

ORNL-DWG 83-2446A FED

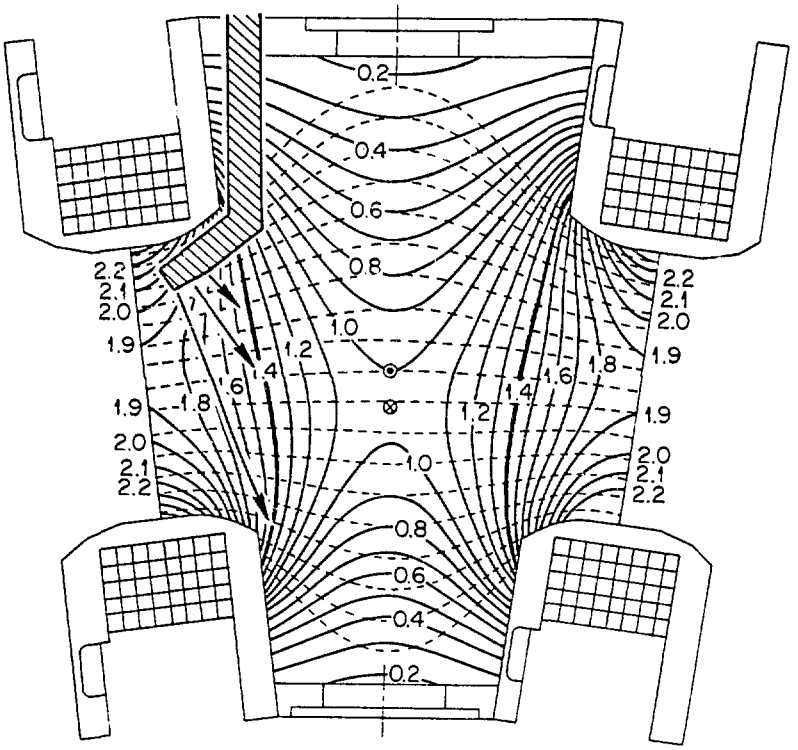

Fig. 4

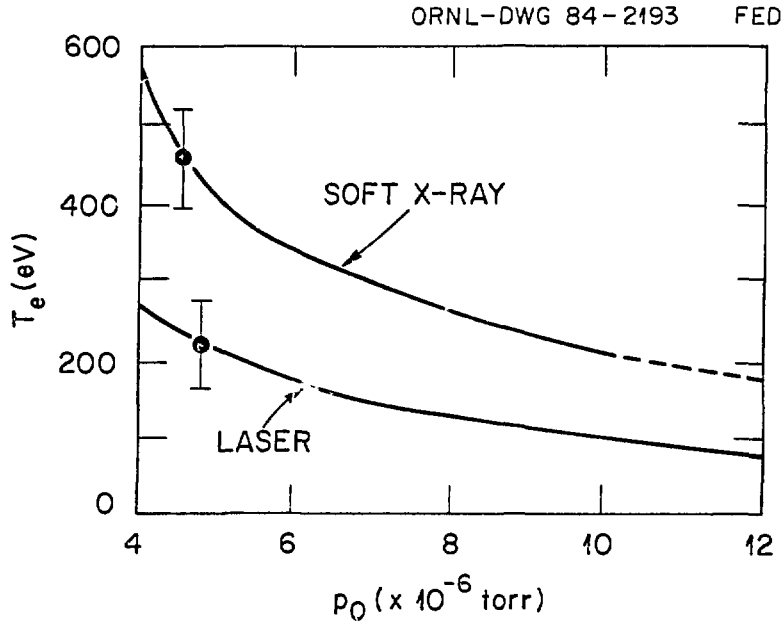
ORNL-DWG 84-2193 FED
600
400
200
0
T_e (eV)
SOFT X-RAY
LASER
4
6
8
10
12
p_O (x 10^{-6} torr)

Fig. 5

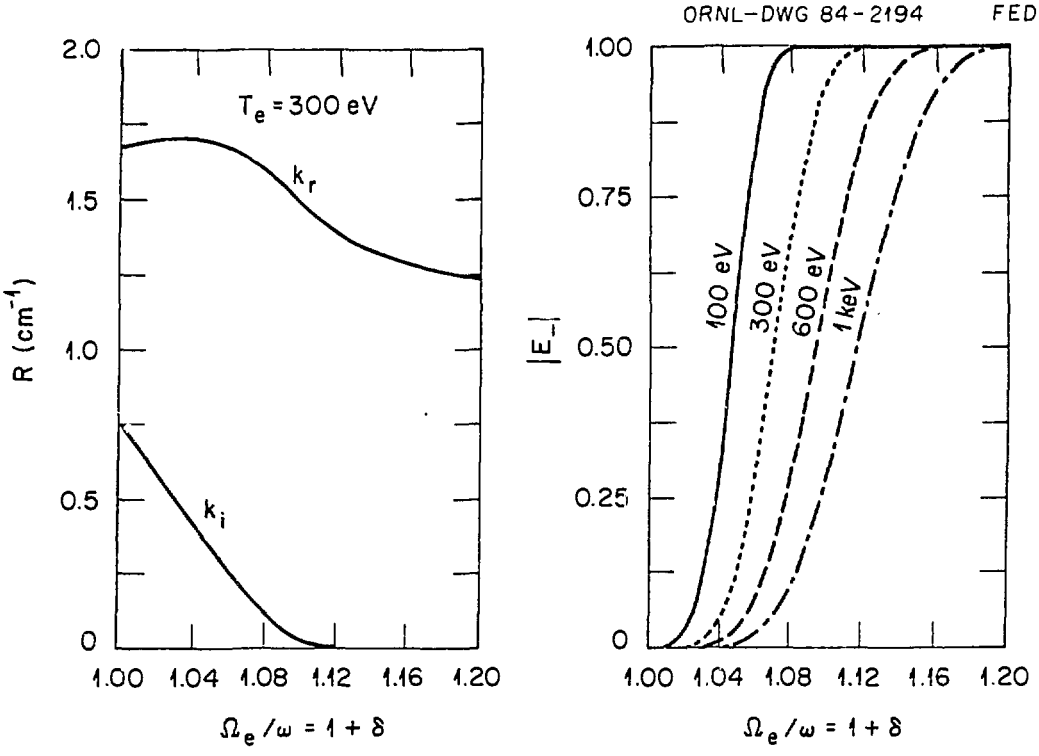
ORNL-DWG 84-2194 FED
2.0
1.5
1.0
0.5
0
R (cm^{-1})
T_e = 300 eV
k_r
k_i
1.00 1.04 1.08 1.12 1.16 1.20
$\Omega_e/\omega = 1 + \delta$
1.00
0.75
0.50
0.25
0
$|E_-|$
100 eV
300 eV
600 eV
1 keV
1.00 1.04 1.08 1.12 1.16 1.20
$\Omega_e/\omega = 1 + \delta$

Fig. 6

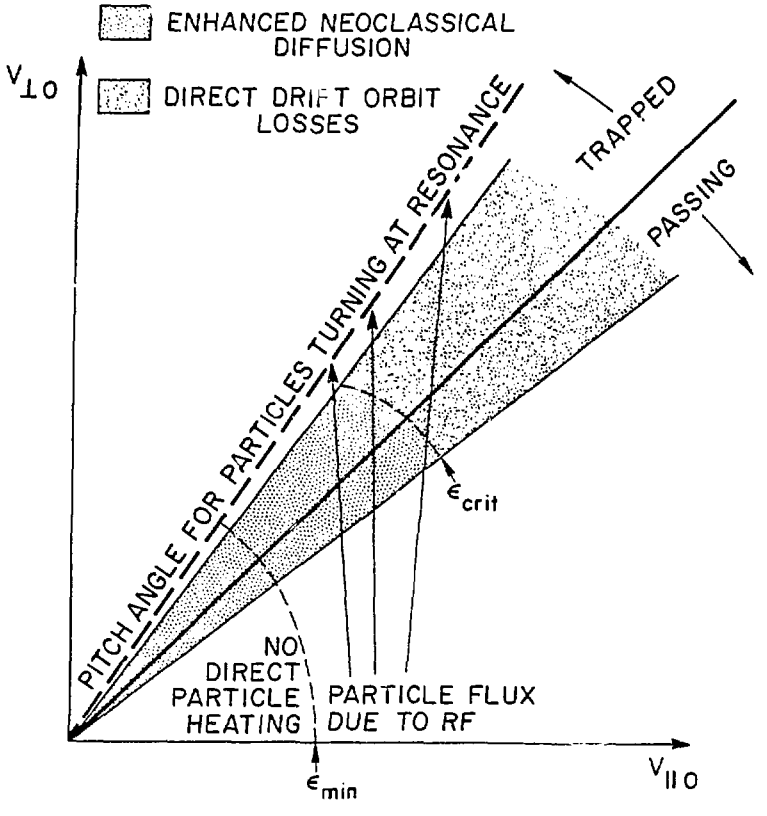
ENHANCED NEOCLASSICAL DIFFUSION
DIRECT DRIFT ORBIT LOSSES
$V_{\perp 0}$
TRAPPED
PASSING
PITCH ANGLE FOR PARTICLES TURNING AT RESONANCE
ϵ_{crit}
NO DIRECT PARTICLE HEATING
PARTICLE FLUX DUE TO RF
ϵ_{min}
$V_{\parallel 0}$

Fig. 7